Structure–properties correlation in (1-x)$Bi_{0.90}Pr_{0.10}FeO_3$ - (x)$Ca_{0.5}Sr_{0.5}TiO_3$: Phase evolution, optical, and electrical properties

J.R.D. Ruiz López[a], V.E. Alvarez-Montano[b], Francisco Brown[a], Sunil Chauhan[c], Oscar Raymond Herrera[d], Subhash Sharma[*de]

[a] Universidad de Sonora, Departamento de Investigación en Polímeros y Materiales, Rosales y Luis Encinas s/n col. Centro, Hermosillo, Sonora 83000, México.

[b] Universidad de Sonora, Departamento de Ingeniería Química y Metalurgia, Rosales y Luis Encinas s/n col. Centro, Hermosillo, Sonora 83000, México.

[c] Department of Physics & Environmental Sciences, Sharda School of Engineering & Science, Sharda University, Uttar Pradesh 201310, India

[d] Centro de Nanociencias y Nanotecnología. Universidad Nacional Autónoma de México, Km 107 Carretera Tijuana-Ensenada, AP 14, Ensenada 22860, B.C., México.

[e] SECIHTI - Centro de Nanociencias y Nanotecnología, Universidad Nacional Autónoma de México, Km. 107 Carretera Tijuana-Ensenada, AP 14, Ensenada 22860, B.C., México.

Corresponding author: subhash@ens.cnyn.unam.mx

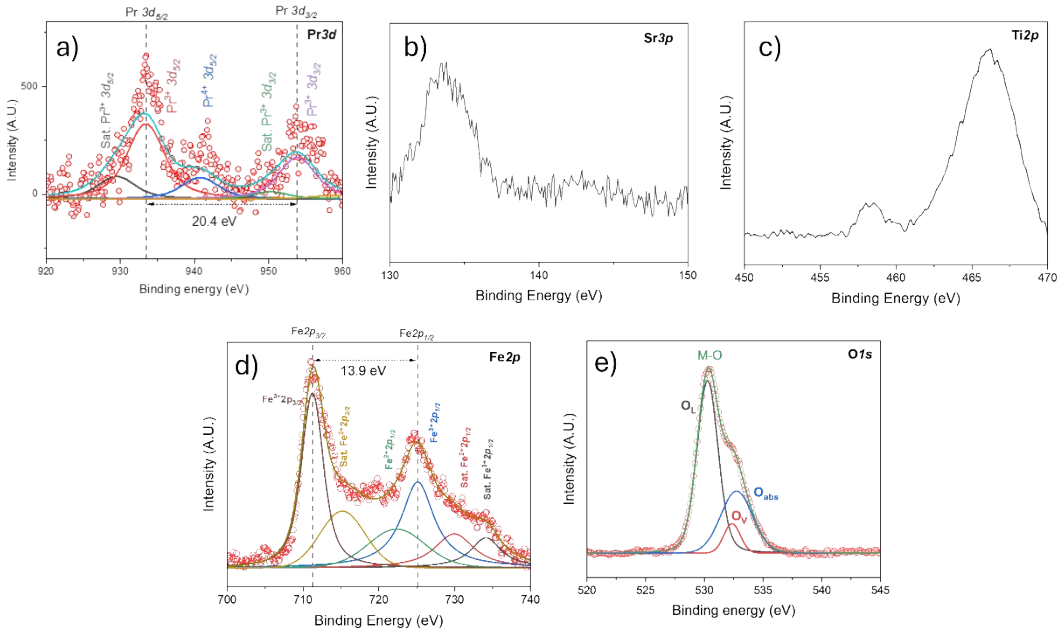

Fig. SF1: High-resolution XPS spectrum of the (1–x)$Bi_{0.9}Pr_{0.1}FeO_3$–x$Ca_{0.5}Sr_{0.5}TiO_3$ sample x = 0.15 measured for (a) Pr 3d, (b) Sr 3p (c) Fe 2p, (d) Ti 2p and (e) O 1s core levels

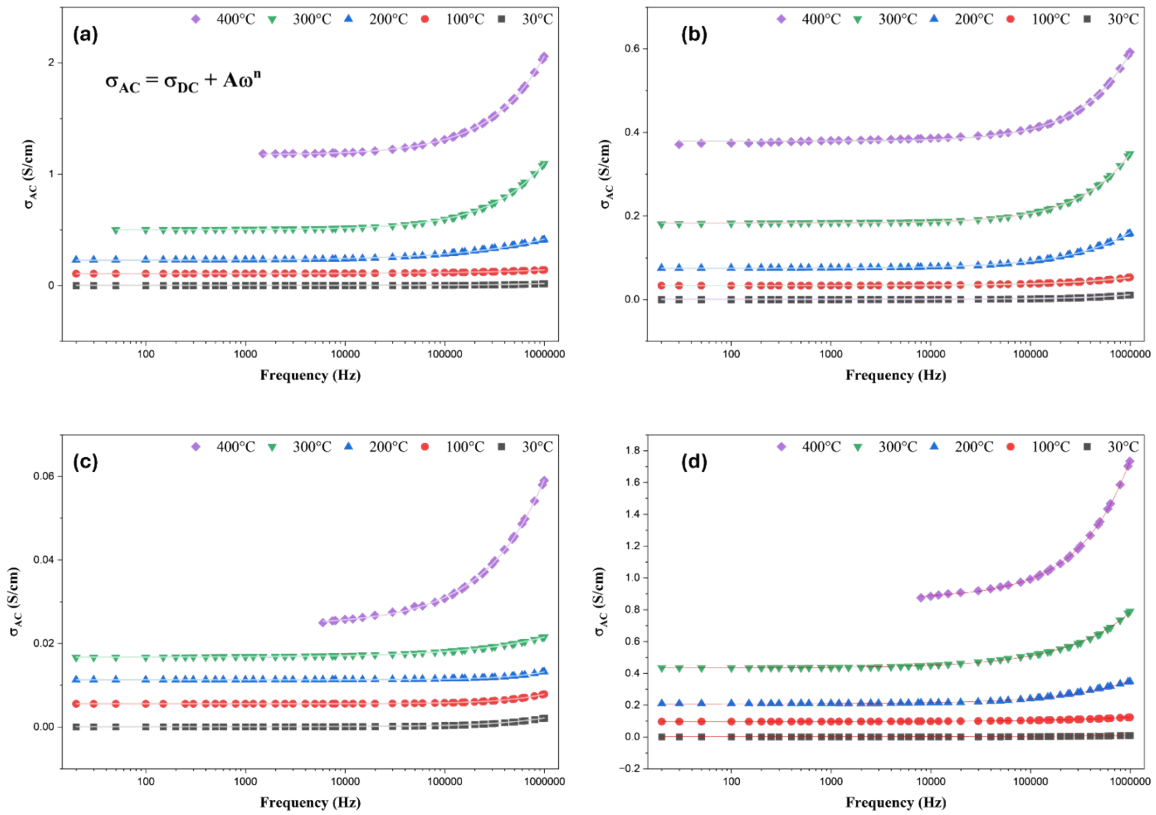

Fig. SF2: Fitting of the conductivity σ_{AC} by the Jonscher power law for (1-x)BPFO-xCSTO, x = 0.0, 0.05, 0.10, and 0.15.

Table S1: Binding energies from Bi 4f, Fe 2p, and Pr 3d core levels for x = 0.00

Element	Level	Oxidation number	B.E (eV)
Bi	$4f_{7/2}$	3	159.4
	$4f_{5/2}$	3	164.7
Fe	$2p_{3/2}$	3	711.1
	Sat. $2p_{3/2}$	3	718.8
	Sat. $2p_{3/2}$	2	714.2
	$2p_{1/2}$	3	724.8
	Sat. $2p_{1/2}$	2	727.7
Pr	Sat. $3d_{5/2}$	3	930.2
	$3d_{5/2}$	3	933.8
	$3d_{5/2}$	4	940.1
	Sat. $3d_{3/2}$	3	949.7
	$3d_{3/2}$	3	953.9
	$3d_{3/2}$	4	957.7

Table S2: Binding energies from Bi 4f and Fe 2p core levels.

Element	Level	Oxidation number	B.E (eV)
Bi	$4f_{7/2}$	3	159.4
	$4f_{5/2}$	3	164.7
Fe	$2p_{3/2}$	3	711.2
	Sat. $2p_{3/2}$	2	715.2
	$2p_{1/2}$	2	722.3
	$2p_{1/2}$	3	725.1
	Sat. $2p_{1/2}$	2	729.9
	Sat. $2p_{1/2}$	3	734.1
Pr	Sat. $3d_{5/2}$	3	929.5
	$3d_{5/2}$	3	933.4
	$3d_{5/2}$	4	940.7
	Sat. $3d_{3/2}$	3	950.2
	$3d_{3/2}$	3	953.8
	$3d_{3/2}$	4	958.3

Table S3. Fitting parameters obtained from Jonscher's power law fitting at different temperatures.

	x = 0.0			**x = 0.05**		
Temperature (°C)	**$\sigma_{D.C}$ (S/cm)**	**A**	**n**	**$\sigma_{D.C}$ (S/cm)**	**A**	**n**
30	3.16E-04	6.05E-08	0.7989	3.43E-05	2.43E-08	0.83066
100	0.00137	6.84E-06	0.5445	5.17E-05	8.79E-07	0.63926
200	0.03519	5.58E-05	0.5202	0.0047	1.42E-06	0.70282
300	0.5565	2.52E-06	0.7909	0.12572	2.69E-08	0.85202
400	4.10544	2.90E-07	0.807	1.1309	2.46E-07	0.8727
	x = 0.10			**x = 0.15**		
Temperature (°C)	**$\sigma_{D.C}$ (S/cm)**	**A**	**n**	**$\sigma_{D.C}$ (S/cm)**	**A**	**N**
30	1.77E-05	6.13E-09	0.8138	-6.83E-06	7.49E-07	0.60073
100	7.40E-06	3.16E-10	1.0093	-2.21E-04	4.35E-06	0.55868
200	5.97E-05	2.08E-10	1.0233	-0.00113	7.15E-06	0.63377
300	4.33E-04	9.04E-07	0.548	0.04246	9.95E-06	0.66842
400	0.12542	4.11E-07	0.7249	2.13887	1.52E-06	0.84646

Table S4. Physical properties comparison with reported literature.

Properties	In this study	Reported in lit.	Comments
ε_r	~79.09 – 84.00 (0.00-0.15) **(RT, 100KHz)**	~85 (from 1KHz to 1GHz), ~90 (from 100KHz to 800MHz) (BFO-$BaZrO_3$, BFO-$CaTiO_3$, respectively) [1]	BFO-ABO_3-type ceramics were fabricated with a conventional method.
		~26-36 (observed at 100KHz and above) [2]	BFO films were prepared by a chemical solution route.
		~120 (100KHz) [3]	Dielectric properties of pure polycrystalline BFO obtained by the solid-state reaction route, heating at 800°C for 48 h.
		~60 (at 100KHz) [4]	$Bi_{1-x}Ba_xFe_{1-y}Co_yO_3$ was synthesized by the solid-state route method.
		46 and 73 (BFO and BFO-$BiMnO_3$, respectively, at 100KHZ) [5]	BFO/$BiMnO_3$ composite ceramics obtained by the sol-gel technique.
E_g (eV)	2.09-2.21	2.02–2.27 [6]	(x-1)BFO-x$SmFeO_3$ ceramics synthesized by solid-state reaction. The Eg value decreased as x decreased.
		1.93 [7]	Ca-Hf co-doped BFO was synthesized by using the sol-gel technique.
		1.6 [8]	Ce-doped BFO-$PbTiO_3$ composite ceramics were synthesized by the solid-state reaction method.
		2.26 [9]	0.8BFO-0.2CTO composite synthesized by the sol-gel method
		3.95 [10]	Structured BFO-$PbTiO_3$ thin films synthesized by the Pechini method for multifunctional photovoltaic applications.

Pr and Ti co-substituted $BiFeO_3$ ceramics with $x \leq 0.20$ were synthesized, with structural phase transition from rhombohedral (*R3c*) with $x \leq 0.10$ to orthorhombic (*Pnma*) phase with $0.10 < x \leq 0.20$ [11].

References:

[1] G. Sreenu, M. Alam, D. Fasquelle, and D. Das, "High-frequency dielectric characterization of novel lead-free ferroelectrics," *Journal of Materials Science: Materials in Electronics*, vol. 31, no. 21, pp. 18477–18486, Nov. 2020, doi: 10.1007/s10854-020-04391-7.

[2] S. Portes Dos Reis, F. B. Minussi, and E. B. Araújo, "Thermally activated processes and bias field effects on the electrical properties of BiFeO 3 thin films," *NANOMATERIALS SCIENCE & ENGINEERING*, vol. 2, no. 1, pp. 25–34, 2020, doi: 10.34624/nmse.v2i1.8485.

[3] J. Lu *et al.*, "On the room temperature multiferroic BiFeO3: magnetic, dielectric and thermal properties," *Eur Phys J B*, vol. 75, no. 4, pp. 451–460, Jun. 2010, doi: 10.1140/epjb/e2010-00170-x.

[4] D. Varshney, A. Kumar, and K. Verma, "Effect of A site and B site doping on structural, thermal, and dielectric properties of BiFeO3 ceramics," *J Alloys Compd*, vol. 509, no. 33, pp. 8421–8426, Aug. 2011, doi: 10.1016/j.jallcom.2011.05.106.

[5] W. A. Wani, P. Mitra, K. Ramaswamy, and H. Venkataraman, "Investigations on structural, morphological, dielectric, and ferroelectric properties of $BiFeO_3$ /$BiMnO_3$ composite ceramics prepared via sol–gel synthesis route," *Ferroelectrics*, vol. 615, no. 1, pp. 67–80, Oct. 2023, doi: 10.1080/00150193.2023.2243564.

[6] C. Rout, S. Pattanayak, and D. Pattanayak, "Investigation on optical and magnetic properties of BiFeO3–SmFeO3 solid solution," *Applied Physics A*, vol. 130, no. 3, p. 165, Mar. 2024, doi: 10.1007/s00339-024-07307-y.

[7] P. Yadav, A. Pandey, B. Khan, R. Biswal, P. Kumar, and M. K. Singh, "Rietveld refinement, dielectric, magneto-dielectric effect and optical properties of (Ca/Hf) co-doped Bisumth ferrite," *Mater Today Proc*, vol. 82, pp. 227–233, 2023, doi: 10.1016/j.matpr.2023.01.121.

[8] S. K. Parida, "Influence of cerium substitution on structural and dielectric properties of the modified $BiFeO_3$ -$PbTiO_3$ ceramics," *Ferroelectrics*, vol. 583, no. 1, pp. 19–32, Oct. 2021, doi: 10.1080/00150193.2021.1980341.

[9] B. Khan, M. K. Singh, P. Yadav, A. Kumar, G. Singh, and P. Kumar, "Optical properties, dielectric relaxor behavior, impedance and modulus spectroscopy of 0.8BiFeO3-0.2CaTiO3 composite," *Mater Chem Phys*, vol. 290, p. 126642, Oct. 2022, doi: 10.1016/j.matchemphys.2022.126642.

[10] V. F. Freitas *et al.*, "On the Characteristics of Perovskite Structured BiFeO3-PbTiO3 Thin Films: Their Potential to Multifunctional Photovoltaic Applications," *Brazilian Journal of Physics*, vol. 51, no. 4, pp. 1215–1223, Aug. 2021, doi: 10.1007/s13538-021-00925-4.

[11] V. Singh, S. Sharma, and R. K. Dwivedi, “Improved dielectric, magnetic and optical properties of Pr and Ti co-substituted BFO ceramics,” *J Alloys Compd*, vol. 747, pp. 611–620, May 2018, doi: 10.1016/j.jallcom.2018.02.120.